ISSN 2278-3091
Volume 9 No.2, March -April 2020
International Journal of Advanced Trends in Computer Science and Engineering
Available Online at http://www.warse.org/IJATCSE/static/pdf/file/ijatcse33922020.pdf
https://doi.org/10.30534/ijatcse/2020/33922020

Method of sustainable detection of augmented reality markers by changing deconvolution

Ihor Ruban[1], Nataliia Bolohova[1], Vitalii Martovytskyi [1], Nataliia Lukova-Chuiko [2], Valentyn Lebediev[1]
[1]Kharkiv National University of Radio Electronics, Ukraine, Kharkiv, 61166,
Nauki ave., 14, dec@nure.ua
[2]Taras Shevchenko National University of Kyiv, Ukraine, Kyiv, 01601,
Str. Volodymyrska, 64/13, lukova@ukr.net

ABSTRACT

The article is devoted to assessing the effectiveness of detection of augmented reality markers after applying blind deconvolution over frames received from the camera of a mobile device. The development and implementation of algorithms for eliminating various interference, artifacts and distortions, as well as testing and comparison of detection algorithms for special points before applying algorithms for eliminating various interference, artifacts and distortions were applied. The following conclusions can be drawn from the experiment. When using general SIFT, SURF recognition methods using image recovery methods (deconvolution), you can notice significant increase in recognition quality with a relatively small increase in operating time.

Key words: virtual reality, aaugmented reality, SIFT, SURF, deconvolution, convolution, blurry image, false acceptance rate, false rejection rate, multidimensional, microcomputer.

1. INTRODUCTION

One of the most popular areas figured out by experts in modern information technologies is the development of augmented and virtual reality technologies. Augmented (AR) and virtual reality (VR) technologies, which now are used by companies to improve workflows and change the approach to work with clients.

From the article's material [1], it is possible to single out main areas of human activity where augmented reality can save millions of dollars, and also help people work faster, more accurately and with less effort.

One of the main areas is education. The more visual examples in the learning process, the better the result, and augmented reality makes it even easier to provide this visibility. From the articles [3, 4] follows that over the past four years the number of studies of augmented reality in education has increased. One of the main advantages of AR is that it helps to improve academic performance. However, there is a number of problems in the AR application area, namely usability and frequent technical problems associated with the correct detection of markers.

The second area of application is medicine. In this area, AR-technology has long earned recognition - simulation programs allow students of medical schools to obtain the necessary skills, and already existing surgeons to work out subtle, complex manipulations. The authors in article [4] gave idea of AR and VR use with an emphasis on surgical workplace. The authors [5] talked about the revolution in the field of computer medicine. Moglia and coauthors [6] provided an overview of VR and AR simulators for robotic surgery. Robotic surgery is also another topic for publication in 2015 [7]. Based on published results of AR use in medicine in article [8], we can draw the following conclusions:

- the AR area has been well studied and there is a positive trend in it's application;
- the application is still in its early stages in the field of medicine and is not widely used in clinical practice;
- clinical studies proving the effectiveness of the applied AR technologies are still missing.

The next area of application is the creation of interactive based on AR in organizing remote technical support for hardware and software tools and tools used in production. A sudden accident or breakdown on manufacture can bring enormous losses, and specialist with the necessary qualifications can be located thousand of kilometers away at the head office of the company. To solve these problems, large companies, including transnational structures, began to introduce augmented reality into their work processes.

The next important area of application is the aircraft industry. Fighter pilots have to make quick decisions, so they use special helmets, where the picture of the real world is supplemented by indications of various instruments. High accuracy is also needed in the production of such aircraft, because the cost of error is very high - starting with the pilot's life a ending with financial costs. The article [9] shows that the augmented reality used in aerospace production processes provides faster production, higher quality and reliability of production processes, as well as increasing the competitiveness of a company.

Despite the fact that much has been written about a new area of augmented reality and how it will integrate data into the real world, it is important to remember the limitations of modern technology. Spreading camera phones and growth of

computing resources in mobile devices in recent years are important factors in the development of software for augmented reality. Nevertheless, the technology of currently located on the smartphones market has not been developed taking into account augmented reality, therefore, the development of technologies and methods for increasing the efficiency of detection of augmented reality markers is relevant.

In modern sources on augmented reality, there is a lot of new information that will eventually be integrated into the real world, but we should remember that modern technologies have some limitations. One of the important factors in the development of software for augmented reality are smartphones that have a computing resource and a camera. At the moment, the technology of smartphones that is on the market does not have the necessary properties for augmented reality, so the development of technologies and methods for increasing the efficiency of detection of augmented reality markers is relevant.

2. ANALYSIS OF LATEST RESEARCHES AND PUBLICATIONS

To create virtual objects superimposed on real-world scenes, it is necessary to solve the problem of isolating and recognizing image elements in the video sequence that come from the device's camera. In the general case, the solution of the problem is reduced to the determination of point features on images of real-world objects in separate frames. Since the stream of video frames contains complex structured information about the observed scene, a technique is required to extract from the video stream in real time from the device's camera in motion information about the point features of objects, or a technique for extracting a special marker from the image frame, which will allow unambiguous identification this object [10-11].

In the paper[10], comparison of existing methods for recognizing point features, such as SIFT, SURF, and RIFF, was made and their disadvantages are presented. In order to improve the quality of method for recognizing objects with highlighted point features on mobile devices, a technique based on a random binary tree has been proposed. The main idea of the technique is to recognize objects based on Bayes classifier distribution statistics about possible descriptor comparisons. The disadvantage of this technique is that at the detection stage, the alleged singular point is "thrown" over the decision tree, which is built for each image of the recognizable object, taken from different angles and under different conditions.

In the article [12], authors demonstrated how types of markers and their scan angles affect the quality of markers detection. Authors proposed the marker ChromaTags [12] which is a continuation of the AprilTags, where two two-color labels are mixed to maximize the gradient value in the CIELAB color space. Color space conversion reduces number of edges compared to grayscale images, thereby speeding up detection.

In the article [13], a method for increasing the accuracy of tracking 2D marker for augmented reality using the particle filtering technique is considered. The method estimates the rotation and movement of camera by tracking the three-dimensional coordinate system fixed on the plane of the marker, based on the input images captured by the moving camera.

The analysis showed that the range of methods for increasing stability recognition of point features is wide enough and does not provide stable operation of the implemented technology. But not a single method takes into account the fact that images on which it is necessary to recognize special points are subject to various noise, artifacts and distortions.

3. PURPOSE AND OBJECTIVES OF THE STUDY

The aim of the work is to develop a registration-invariant method for detecting augmented reality markers using blind deconvolution over frames received from a mobile device's camera.

To achieve this goal, the following tasks were formed:

- development and implementation of algorithms for eliminating various interference, artifacts and distortions;
- testing and comparison of detection algorithms for special points before applying algorithms to eliminate various interference, artifacts and distortions and after.

4. STATEMENT OF THE PROBLEM OF RESTORING A BLURRY IMAGE

The task of restoring the original image after interference, artifacts and distortion is described in many sources [10–15]. After analyzing the publications, we will consider the generalized image restoration process presented in Figure 1.

Where f(x,y) – source image, h(x,y) – a function representing a distorting operator in the spatial domain, η(x,y) – additive noise

Accordingly, image distortion can be represented by the formula (1).

$$g(x,y) = f(x,y) \otimes h(x,y) + \eta(x,y), \qquad (1)$$

where $\otimes$ – convolution operation.

In the formula (1), a mathematical model for the formation of a distorted image was presented, which is used in most works on the subject of image restoration.

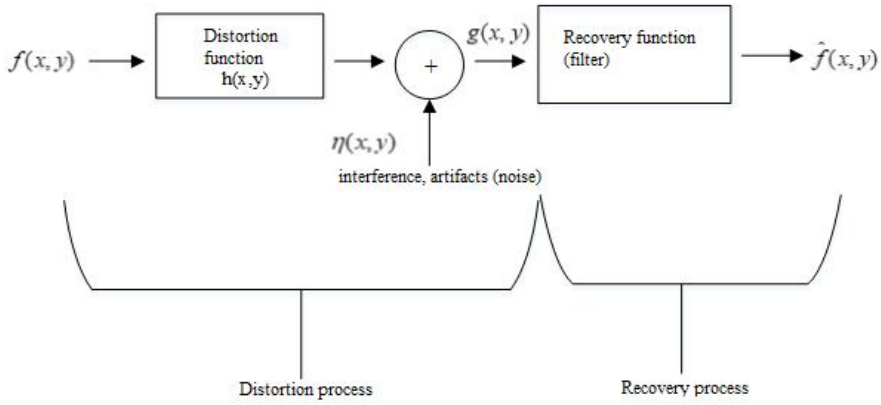

Figure 1: Generalized image recovery process model

In mathematics, the inverse convolution operation is the deconvolution operation. There are many methods for solving the deconvolution operation, examples of which are the method of Wiener and Lucy-Richardson. The advantage of which is the simplicity of implementation, but their main drawback is the presence of known blurring core, which is impossible in real conditions. In this regard, this work will consider such a resolving method as blind deconvolution.
After publications reviewing [12–18], a probabilistic approach using the density function in the form of distribution of a mixture of Gaussian probability density functions will be used to restore the blur core (Mixture of Gaussians = MoG).

5. DESCRIPTION OF WORK OF METHOD OF SUSTAINABLE DETECTION OF AUGMENTED REALITY MARKERS BY USING BLIND DECONVOLUTION

Principle of operation of augmented reality is to combine a virtual object with a video stream from the device's camera. Let us consider in detail the marker detection scheme supplemented with use of deconvolution operation to improve quality of image fed to detector Figure 2.

Since in real conditions the core of blurring image received from the camera of device is not known in advance, the methods of Wiener and Lucy-Richardson cannot be applied in this situation. Therefore, in the scheme of Fig. 2, is proposed to use the pyramidal approach to the restoration of the blurring image core, when the core is gradually restored from low to high resolution. At each step of the restoration of core, the data on the blurring core are refined, and thus it approaches an exact solution. This type of solution is considered in many articles [12, 15, 16]. Figure 3 shows a general view of the core algorithm scheme.

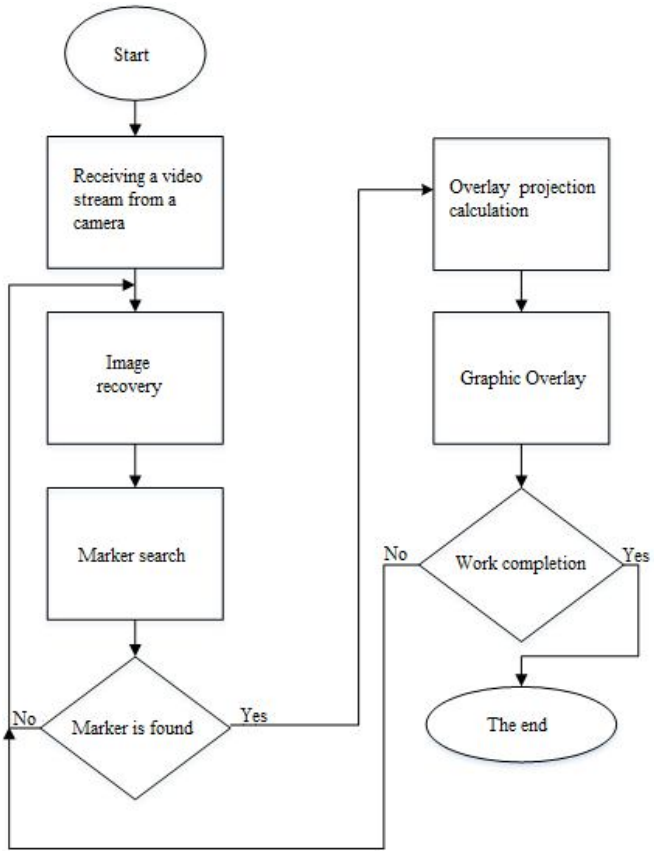

Figure 2: Augmented reality marker definition scheme using deconvolution operation to improve image quality

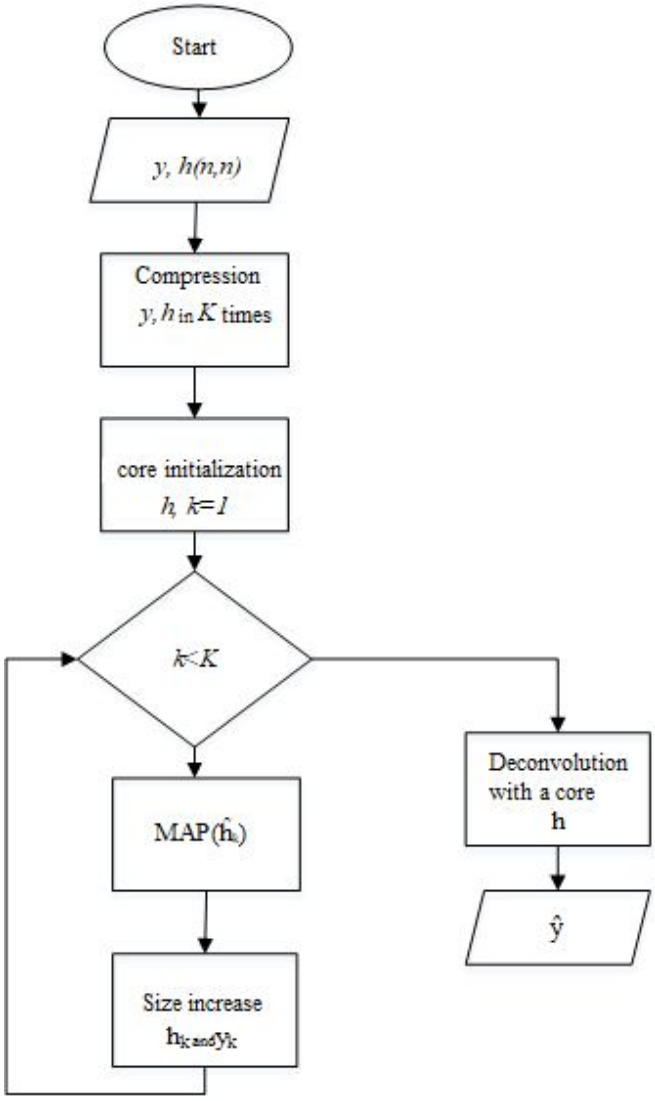

Figure 3: Core recovery algorithm scheme

Input algorithm parameter is *y* – vector representation of the original image, *h(n, n)* – blur core. The next step is compress on at the image and blur core by K times, after which the blurring core is initialized. Next, core is evaluated by method of maximizing the posterior distribution (MAP), considered in detail in the paper[18], maximize the density of the posterior distribution of blur core (2) due to the fact that it has much smaller size than the image itself:

$$\hat{h} = \arg\max_h p(h \mid y) = \arg\max_h p(y \mid h) \quad (2)$$

Conditional distribution p(y|h) of (2) can be written as follows (3).

$$p(y \mid h) = \int p(x, y \mid h) dx \quad (3)$$

Prior distribution p(h) can be omitted in formula (3) due to the assumption that the components of core are uniformly distributed.

A mixture of Gaussian distributions formula (4) was used as an a priori distribution for the original image.

$$p(x) = \prod_i \prod_\gamma \sum_j \frac{\pi_j}{\sqrt{2\pi\sigma_j}} e^{-\frac{1}{2\sigma_j^2}\| f_{i,\gamma}(x)\|^2} \quad (4)$$

In the formula (4) $f_{i,\gamma}(x)$ – convolution result of the i-th pixel, δ_j - standard deviation of the j-th mixture.

Credibility will be presented as follows (5):

$$p(y \mid x, h) = \frac{1}{(\sqrt{2\pi\eta})^N} e - \frac{\| h \otimes x - y \|^2}{2\eta^2} \quad (5)$$

The formula (5) takes into account Gaussian noise with dispersion η^2, N – number of image pixels. Accordingly, a priori can be written as in the publication [14]:

$$p(f_{i,\gamma}(x)) = \sum_j \frac{\pi_j}{\sqrt{2\pi\sigma_j}} e^{-\frac{1}{2\sigma_j^2}\| f_{i,\gamma}(x)\|^2} \quad (6)$$

Due to the fact that joint distribution *p (y, x, h) = p (y, x|h) p (h) = p (y|x, h) p (x) p (h),* conditional distribution taking into account can be written in the form:

p (y, x | h) taking into account (4)(5) and (6) can be written as (7):

$$-\log p(y, x \mid h) = \frac{\| h \otimes x - y \|^2}{2\eta^2} - \sum_{i,\gamma} \log p(f_{i,\gamma}(x)) + c \quad (7)$$

here c is a constant, and h has a uniform distribution, therefore p (h) is omitted.

It is proposed to introduce hidden variables in the model in order to simplify further calculations. Let a discrete hidden variable be introduced $k_{i,j}$, which can take any value from {1,…,□} then the conditional distribution for image can be written as (8):

$$p(f_{i,\gamma}(x)) \mid k_{i,\gamma}) = \sum_j \frac{k_{i,\gamma,j}}{\sqrt{2\pi\sigma_j}} e^{-\frac{1}{2\sigma_j^2}\| f_{i,\gamma}(x)\|^2} \quad (8)$$

Priori distribution for hidden variables (8) will be equal to:

$$p(k_{i,\gamma} = j) = \pi_j \quad (9)$$

Given the hidden variables, a priori distribution for the gradients (discrete derivatives) of image will be written as follows (10):

$$p\left(f_{i,\gamma}(x)\right)=\sum_j \pi_j p\left(f_{i,\gamma}(x)\right)|k_{i,\gamma})=\sum_j \frac{\pi_j}{\sqrt{2\pi\sigma_j}} e^{-\frac{1}{2\sigma_j^2}\| f_{i,\gamma}(x)\|^2} \quad (10)$$

Expression (7) with the input of hidden variables k will be written as follows:

$$\begin{aligned} -\log p(y,x,k\mid h) &= \frac{\| h\otimes x-y\|^2}{2\eta^2} + \\ +\sum_{i,j,\gamma} k_{i,j,\gamma}&\left(\frac{\| f_{i,\gamma}(x)\|^2}{2\sigma_j^2}+\frac{1}{2}\log(\sigma_j^2)-\log(\pi_j)\right)+c \end{aligned} \quad (11)$$

The algorithm uses Bayesian variational derivation to find the posterior distribution of hidden (clean) image p(x|y, h). The idea of Bayesian variational derivation here is to approximate the distribution p(x|y, h) distribution q(x) to simplify the calculation. New distribution (12) will look like this:

$$q(x,k)=q(x)\prod_{i,\gamma} q(k_{i,\gamma}) \quad (12)$$

In the formula (12) *q(x)* – gaussian distribution, which is characterized by mathematical expectation μ and covariance matrix *C*. Thus, you need to know two parameters to determine this distribution. Distribution $q(k_{i,\gamma})$ – *J*–dimensional vector which elements sum to 1, where *j*–th vector element – $p(k_{i,\gamma}=j)$.

Next, you need to rewrite the expression for the lower bound *L(q)*:

$$\begin{aligned} L(q)&=\int q(x,k)\log p(y,x,k\mid h)dkdx - \\ -&\int q(x,k)\log q(x,k)dkdx \end{aligned} \quad (13)$$

Formula (13) can also be represented in the form (14):

$$L(q)=-KL(q(x,k)\parallel p(x,k\mid y,h))+\log p(y\mid h) \quad (14)$$

It is necessary to maximize the functional L (q) from (14) in order to find solution.

For the current task of image restoration, taking into account all the hidden variables introduced, the expression for L (q) will be written in the form (15):

$$\begin{aligned} L(q)=&-\int q(x)\left(\frac{\| h\otimes x-y\|^2}{2\eta^2}+\sum_{i,\gamma,j} q(k_{i,\gamma,j})\frac{\| f_{i,\gamma}(x)\|^2}{2\sigma^2}\right)dx - \\ -&\sum_{i,\gamma,j} q(k_{i,\gamma,j})\left(\frac{1}{2}\log\left(\sigma_j^2\right)\right)-\log\left(\pi_j\right)+\log\left(q\left(k_{i,\gamma,j}\right)\right)+\frac{1}{2}\log|C|+c \end{aligned} \quad (15)$$

Expression (15) must be minimized for each of the variables μ and *C*, $q(\kappa_{i,\gamma})$.

To minimize expression (15) with respect to the parameter $q(k_{i,\gamma})$ parameters μ, *C*, □ are fixed and stand out from the formula (15) members with $q(k_{i,\gamma})$ and we have the following formula:

$$\sum_j (k_{i,\gamma,j})\left(\frac{\mathrm{E}[\| f_{i,\gamma}(x)\|^2]}{2\sigma_j^2}+\frac{1}{2}\log\left(\sigma_j^2\right)-\log\left(\pi_j\right)+\log(q(k_{i,\gamma,j}))\right) \quad (16)$$

In (16) the expression $E[\| f_{i,j}(x)\|^2]=\int(q(x)\| f_{i,j}(x)\|^2)dx$ can be calculated using μ and *C*:

$$\mathrm{E}\left[\| f_{i,j}(x)\|^2\right]=\mu[i]^2+C[i,i] \quad (17)$$

Expression (16) must be minimized by $q(k_{i,\gamma})$. Vector $q(k_{i,\gamma})$ should be *J* – measured and unit amount. Expression for $q(k_{i,\gamma})$ (18) can be written as:

$$q\left(k_{i,\gamma,j}\right)=\frac{\pi_j}{\sigma_j} e^{-\frac{\mathrm{E}[\| f_{i,\gamma}(x)\|^2]}{2\sigma_j^2}} \quad (18)$$

In (18), formula was obtained by which expression (16) is minimized, which was the task of updating the parameter $q(k_{i,\gamma})$.

To minimize the expression (15) to the parameter μ, it is necessary to fix the variables in formula (15), and also leave all the members, containing x.

First you need to rewrite expression (7) in the form (19):

$$\begin{aligned} &-\log p(y,x\mid h)= \\ &=\frac{\| h\otimes x-y\|^2}{2\eta^2}-\sum_{i,\gamma}\frac{\| f_{i,\gamma}(x)\|^2}{2\sigma^2}+c= \\ &=\frac{1}{2}x^T A_x x-b_x^T x+c \end{aligned} \quad (19)$$

In expression (19), c is a constant, the remaining members ((20)-(21)):

$$A_x=\frac{1}{\eta^2}T_h^T T_h+\frac{1}{\sigma^2}\sum_\gamma T_{f_\gamma}^T T_{f_\gamma} \quad (20)$$

$$b_x=\frac{1}{\eta^2}T_h^T y \quad (21)$$

In expressions (20) and (21) $T_Ø$ denotes a filter matrix Ø (in this case, the discrete derivative). Conditional distribution *p(x|y,h)* is Gaussian, its mathematical expectation and covariance matrix (22) can be written as follows:

$$C=\mathrm{A}_x^{-1}\quad \mu=Cb_x \quad (22)$$

From the expression (22) it is clear that μ is a solution A_x $\mu=b_x$. Taking into account expressions (19), (20), (21), (22) and introducing additional hidden variables into the model as a distribution $q(k_{i,\gamma})$ expression (15) will be written as (23):

$$L(q) = -\int q(x)\left(\frac{1}{2}x^{T} A_x x - b_x^T x\right)dx + \frac{1}{2}\log|C| + c \tag{23}$$

Due to the adding of additional hidden variables, expression (20) will be represented as (24):

$$A_x = \frac{1}{\eta^2}T_h^T T_h + \sum_{\gamma} T_{f_\gamma}^T W_\gamma T_{f\gamma} \tag{24}$$

where W_γ is a diagonal matrix with the following elements (see (25)):

In (24) $\omega_{i,\gamma,j}=q(k_{i,\gamma,j})$ can be calculated from expression (17). The integral from (22) can be calculated (25):

$$L(q) = -\frac{1}{2}\mu^T A_x \mu + b_x^T \mu - \frac{1}{2}Tr(A_x C) + \frac{1}{2}\log|C| + c \tag{25}$$

In (25) Tr(·) denotes the trace of the matrix. Since equation (25) is quadratic in μ, then minimization (25) can be reduced to solving a system of linear equations (see (25))

$$A_x \mu = b_x \tag{25}$$

To update parameter C, the covariance matrix is proposed to set to diagonal (27), where its element will be calculated as:

$$C[i,i] = \frac{1}{A_x[i,i]} \tag{27}$$

Thus, the covariance matrix can be calculated in just O (N) operations.

After calculating μ, C should update core blur. To do this, it's necessary to minimize the expression $E_q\left[\|h \otimes x - y\|^2\right]$, which reduces to solve quadratic programming problem (28):

$$\min_h \tfrac{1}{2}h^T \overline{A_h} h - \overline{b}_h^T h, \;\; s.t. h \geq 0 \tag{28}$$

where in (28):

$$\overline{A_h}[i_1 i_2] = \sum_i \mu[i+i_1]\mu[i+i_2] + C[i+i_1, i+i_2] \tag{29}$$

$$\overline{b_h}[i_1] = \sum_i \mu[i+i_1]y[i] \tag{30}$$

This will be true since the expression $\|h \otimes x - y\|^2$ is quadratic in h; therefore, it can be written as $\|h \otimes x - y\|^2 = h^T A_h h - b_h^T h$, in which for size h equal to the matrix $m \times m$, $M=m^2$ matrix A_h (31) will be sized $M \times M$:

$$A_h[i_1, i_2] = \sum_i x[i+i_1] \times [i+i_2] \tag{31}$$

$$b_h[i_1] = \sum x[i+i_1]y[i] \tag{32}$$

In the above formulas i runs through all the pixels in the image, i_1, i_2 - core indices. Averaging expressions (20), (31) over x values, taking into account the distribution q (x), gives the averaged expressions (28), (29). Expression (27) is a quadratic programming problem and can be solved by any existing optimization method. After which, by deconvolution with the found core, the source image is found $\tilde{y}$.

6. DISCUSSION OF THE EXPERIMENTAL RESULTS

The following parameter values were chosen for the experiment: Gaussian distribution with standard deviation δ_j = (701.58, 472.11, 49.9) and variables πj = {0.3047, 0.4344, 0.2609}. Standard deviation of Gaussian noise η = 0.01. To evaluate the core, 2 iterations should be used, and 9 iterations are used to evaluate image. Original image size (1536 × 2048) Figure 4.

Figure 4: Source image

After applying the core recovery algorithm, fig. 3 received the following result, fig. 5 and fig. 6.

Figure 5: Recovered image

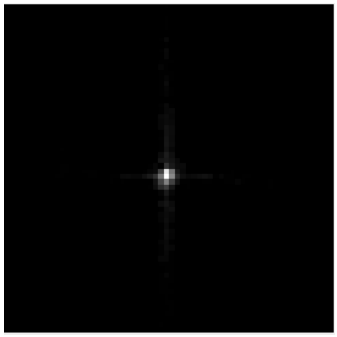

Figure 6: Restored blur core

After that, according to the scheme presented in Fig. 2, comparison of the singular points in the image was made, and the images of various drinks in Fig. 7 were taken as markers.

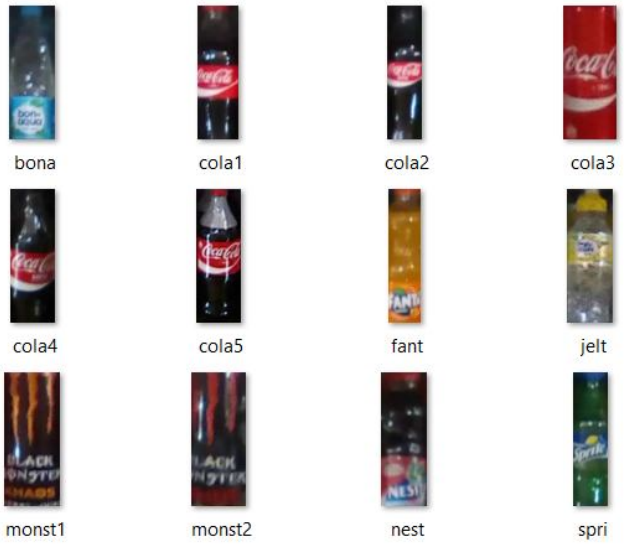

Figure 7: Markers

The number of special image points for detectors 10. The test results are presented in table 1.

Table 1: Marker recognition results

Augmented reality marker definition		Recognition quality, %	Working hours, s.
Classical	SIFT	63	0,5-1
	SURF	74	0,5-1
Modified	SIFT	68	~ 2,5
	SURF	85	~ 2,5

Figure 8 shows an example of matching special points for the original and the restored image.

From figure 8 we can conclude that the preliminary processing of the image to eliminate artifacts has a positive effect on stability of markers detection.

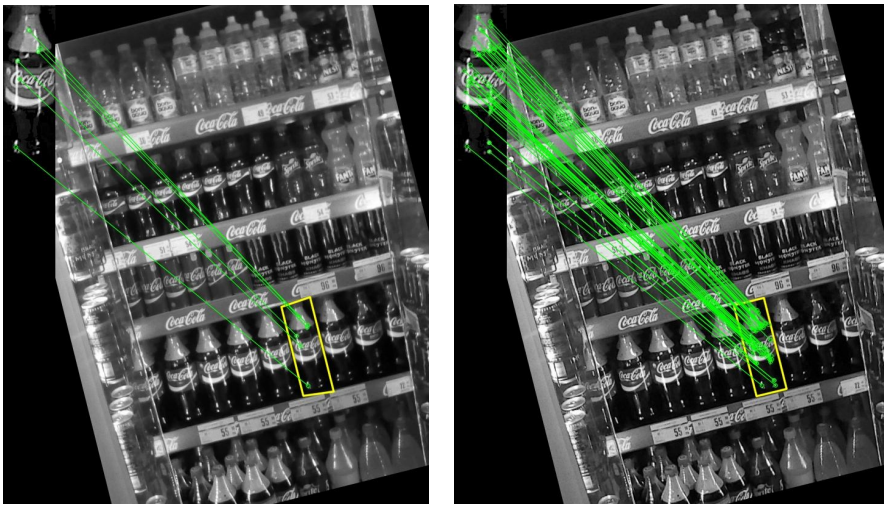

a) b)

Figure 8: Matching special points: a) source image, b) restored image

7.CONCLUSION

The following conclusions can be drawn from the results of the experiment. When using the common SIFT, SURF recognition methods using image recovery methods (deconvolution), you can notice a significant increase in recognition quality with a relatively small increase in operating time.

Based on abovementioned and taking into account the peculiarities of building AR technologies and time spent on data sending, which increases the processing time, the further development of the method should include use of parallel information processing methods to reduce its operation time, as shown in the article [19].

REFERENCES

1. Billinghurst Mark, Adrian Clark, and Gun Lee **A survey of augmented reality,** *Foundations and Trends in Human-Computer Interaction*, vol. 8, no. 2-3, pp. 73-272, 2015.
https://doi.org/10.1016/j.egypro.2015.07.688

2. M. Akçayır, G. Akçayır. **Advantages and challenges associated with augmented reality for education: A systematic review of the literature**, *Educational Research Review*, vol. 20, no. 1, pp. 1-11, February 2017.

3. Chen P., Liu X., Cheng W., & Huang R. ***A review of using Augmented Reality in Education from 2011 to 2016***, *Innovations in smart learning, Springer-Singapore, 2017*, pp. 13-18.
https://doi.org/10.1007/978-981-10-2419-1_2

4. Khor W. S., Baker B., Amin K., Chan A., Patel, K., & Wong, J. **Augmented and virtual reality in surgery-the digital surgical environment: applications, limitations and legal pitfalls**, *Ann Transl Med*, vol. 4, no. 23 pp. 1-10, December 2016.

5. DJ. Thomas. **Augmented reality in surgery: The Computer-Aided Medicine revolution**, *Int J Surg*, vol. 36, pt. A, p. 25, December 2016.
https://doi.org/10.1016/j.ijsu.2016.10.003

6. A. Moglia, V. Ferrari, et al. **A Systematic Review of Virtual Reality Simulators for Robot-assisted Surgery**, *Eur Urol*, vol. 69, no. 6, pp. 1065-1080, Jun 2016.

7. M. Diana, J. Marescaux. **Robotic surgery**, *Br J Surg*, vol. 102, no. 2, pp. e15-e28. January 2015.
https://doi.org/10.1002/bjs.9711

8. M. Eckert, J. S. Volmerg, C. M. Friedrich. **Augmented reality in medicine: systematic and bibliographic review**, *JMIR MHealth and UHealth*, vol. 7, no. 4, p.e10967, April 2019.

9. M. A. Frigo, E. C. C. da Silva, G. F. Barbosa. **Augmented Reality in Aerospace Manufacturing: A Review,** *Journal of Industrial and Intelligent Information*, vol. 4, no. 2, March 2016.

10. S. Wu et al. **A comprehensive evaluation of local detectors and descriptors**, *Signal Processing: Image Communication*, vol. 59, pp. 150-167, Jul 2017.

11. Khudov, H., Ruban, I., Makoveichuk, O., Pevtsov, H., Khudov, V., Khizhnyak, I., Khudov, R. . **Development of Methods for Determining the Contours of Objects for a Complex Structured Color Image Based on the Ant Colony Optimization Algorithm.** *EUREKA: Physics and Engineering*, (1), 34-47.
https://doi.org/10.21303/2461-4262.2020.001108

12. W. Li et al. **Blind image deconvolution based on robust stable edge prediction,** *IEEE-EMBS International Conference on Biomedical and Health Informatics*,pp. 66-69, April 2016.

13. A. Levin, Y. Weiss, F. Durand, W. T. Freeman. **Efficient Marginal Likelihood Optimization in Blind Deconvolution**, *EEE Conf. on Computer Vision and Pattern Recognition*, pp. 2657-2664, June 2011.

14. H. Kuchuk, A. Kovalenko, B.F. Ibrahim, I. Ruban. **Adaptive compression method for video information**, *International Journal of Advanced Trends in Computer Science and Engineering*, vol. 8, no. 1.2, pp. 66-69, 2019.
https://doi.org/10.30534/ijatcse/2019/1581.52019

15. Ruiz P., Zhou X., Mateos J., Molina R. & Katsaggelos A. K. **Variational Bayesian Blind Image Deconvolution: A review**, *Digital Signal Processing*, vol. 47, pp. 116-127, May 2015.

16. Z. Xu, V. Miguel, Z. Fugen, K. Aggelos, M. Rafael. **Fast Bayesian blind deconvolution with Huber Super Gaussian priors**, *Digital Signal Processing*, vol. 60, pp. 122-133, January 2017.
https://doi.org/10.1016/j.dsp.2016.08.008

17. J. Portilla, V. Strela, M. J. Wainwright, E. P. Simoncelli. **Image Denoising Using Scale Mixtures of Gaussians in the Wavelet Domain**, *IEEE Trans. on Image Processing*, vol. 12, no. 11, pp. 1388-1351, October 2003.

18. Smelyakov K., Sandrkin D., Ruban I., Martovytskyi V., & Romanenkov Y. **Search by image. New search engine service model,** *International Scientific-Practical Conference Problems of Infocommunications. Science and Technology*, pp. 181-186, October 2018.

19. V. Diachenko, O. Liashenko, B. Fareed Ibrahim, Oleg Mikhal, Y. Koltun**. Kohonen Network with Parallel Training: Operation Structure and Algorithm**, *International Journal of Advanced Trends in Computer Science and Engineering*, Volume 8, No.1.2, 2019.
https://doi.org/10.30534/ijatcse/2019/0681.22019